ADVANCED FUNCTIONAL MATERIALS
www.afm-journal.de

Printing Hydrogels and Elastomers in Arbitrary Sequence with Strong Adhesion

Hang Yang, Chenghai Li, Meng Yang, Yudong Pan, Qianfeng Yin, Jingda Tang, Hang Jerry Qi, and Zhigang Suo**

Many recently demonstrated devices require the integration of hydrogels and hydrophobic elastomers. Extrusion print is a promising method for rapid prototyping but existing approaches do not fulfill a basic requirement: print integrated structures of a hydrogel and an elastomer, in arbitrary sequence, with strong adhesion. This paper demonstrates an approach to fulfill this requirement. During print, the ink of each material flows through a nozzle under a pressure gradient but retains the shape against gravity and capillarity. During cure, covalent bonds form to link monomer units into polymer chains, crosslink the polymer chains into the polymer networks of the hydrogel and the elastomer, as well as interlink the two polymer networks into an integrated structure. The approach covalently interlinks the hydrogel network and the elastomer network by adding an interlink initiator in one of the inks. An adhesion energy above 5000 J m^{-2} is demonstrated. Printed morphing structures survive swelling and printed artificial axons survive repeated hits of a hammer. This approach opens a road to the development of soft devices for broad applications in medicine and engineering.

1. Introduction

Hydrophilic–hydrophobic hybrids are ubiquitous in life. Examples include cactus, watermelon, gut, and axon. In a myelinated axon, for instance, the cytoplasm and extracellular matrix are hydrophilic and conduct electricity, whereas the myelin sheath is hydrophobic and insulates electricity. The integration of the hydrophilic and hydrophobic substances enables the myelinated axon to function as a transmission line of electrical signals.[1] In recent years, this biological design has inspired the development of synthetic hydrophilic–hydrophobic hybrids, many of which using hydrogels and hydrophobic elastomers to create ionic devices.[2,3] Examples include transparent loudspeakers,[4] transparent membranes for active noise cancellation,[5] artificial muscles,[6,7] artificial axons,[8,9] artificial skins,[10] ionotronic luminescence,[11,12] soft touchpads,[13,14] triboelectric generators,[15–18] stretchable liquid crystal devices,[19] and artificial fish.[20] Hydrogels and hydrophobic elastomers are both soft materials, but it is their dissimilarity that makes these devices functional. Hydrogels transmit electricity and matter, whereas elastomers block them. Hydrogels function as electrodes,[2–4,13] drug delivery media,[21,22] matrices for living devices,[23] and biocompatible coatings.[24–26] Hydrophobic elastomers function as dielectrics[4] and seals.[10,27,28]

Extrusion print is a method of choice for rapid prototyping integrated structures of dissimilar materials.[29–31] Existing approaches, however, do not fulfill a basic requirement: print integrated structures of hydrogels and elastomers, in arbitrary sequence, with strong adhesion. By strong adhesion here we mean that the adhesion energy is comparable to the fracture energy of at least one of the adherends. For example, if the elastomer is tougher than the hydrogel, the adhesion is said to be strong when the adhesion energy is comparable to the fracture energy of the hydrogel. The fracture energy of a widely used hydrogel, polyacrylamide, is on the order of 100 J m^{-2}, and many other hydrogels have achieved fracture energy above 1000 J m^{-2}.[32–35] The abundance of water in a hydrogel creates a challenge. The water molecules in the hydrogel change neighbors readily and transmit little forces, so that the hydrogel usually does not adhere well to any material, not even to another piece of the same hydrogel; the adhesion energy is typically on the order of 1 J m^{-2}.[36] To achieve strong adhesion without hardening the materials, strong but sparse interlinks between the networks of the hydrogel and the elastomer are required, with the strength and density of the interlinks being comparable to those of the crosslinks in the network of the hydrogel or the

H. Yang, C. Li, M. Yang, Y. Pan, Q. Yin, Dr. J. Tang
State Key Laboratory for Strength and Vibration of Mechanical Structures
International Center for Applied Mechanics
Department of Engineering Mechanics
Xi'an Jiaotong University
Xi'an 710049, China
E-mail: tangjd@xjtu.edu.cn
Prof. H. J. Qi
The George W. Woodruff School of Mechanical Engineering
Georgia Institute of Technology
Atlanta, GA 30332, USA
Prof. Z. Suo
School of Engineering and Applied Science
Kavli Institute for Bionano Science and Technology
Harvard University
Cambridge, MA 02138, USA
E-mail: suo@seas.harvard.edu
The ORCID identification number(s) for the author(s) of this article can be found under https://doi.org/10.1002/adfm.201901721.

DOI: 10.1002/adfm.201901721

elastomer. Strong and stretchable hydrogel–elastomer adhesion has been achieved in following steps: 1) preform the elastomer network, 2) modify the elastomer surface (e.g., with oxygen plasma and silanes,[37–40] photoinitiators,[24–27,41] or thermoinitiators[25]), and 3) induce covalent interlinks between the elastomer network preformed with the hydrogel network formed in situ.[25,27] These methods of surface modification, however, cannot be used to print 3D integrated structures in general, where both the elastomer precursor and hydrogel precursor need be printed in arbitrary sequence.[42] Existing prints of a hydrogel and an elastomer in arbitrary sequence do not have the requisite chemistry for strong adhesion but rely on physical interactions, so that the adhesion energy is much below the fracture energy of the hydrogel.[43–46] A recent attempt uses silanes to modify the precursors of elastomers and hydrogels but has yet demonstrated tough and adherent prints.[42]

Here we describe an approach to print integrated structures of a hydrogel and an elastomer, in arbitrary sequence, with covalent crosslink within the networks of the hydrogel and the elastomer as well as covalent interlinks between the two networks. The inks—the precursors of the hydrogel and the elastomer—are designed to fulfill several functions. During print, each ink has the rheology of a plastic liquid like toothpaste, flowing through a nozzle under a pressure gradient, but retaining shape against gravity and capillarity (**Figure 1**a). During cure, covalent bonds form to link monomer units into polymer chains, crosslink polymer chains into polymer networks of the hydrogel and the elastomer, and interlink the two polymer networks into an integrated structure (Figure 1b). In particular, one of the inks carries an initiator to induce, during cure, the formation of the covalent interlinks between the two networks. That is, we add an interlink initiator in the volume of a precursor, not on the surface of a preformed network. We print integrated structures of high fracture energies (≈10 000 J m^{-2} for the hydrogel and ≈6000 J m^{-2} for the elastomer) as well as high adhesion energy (≈5000 J m^{-2}). The printed morphing structures survive swelling and the printed artificial axons survive repeated hits of a hammer.

2. Results and Discussion

It is conceivable that this general approach can be realized using various chemistries. This paper uses a specific set of chemistries. We prepare the ink for a microgel-reinforced hydrogel (poly(2-acrylamido-2-methyl-1-propanesulfonic sodium) (PNaAMPS) microgels, polyacrylamide matrix). The networks of the microgels and the network of the hydrogel matrix interpenetrate in topological entanglement. In fact, there are other candidates of tough hydrogels for printing, For example, the alginate-polyacrylamide hydrogel is tough[35] and printable.[47] However, the alginate-polyacrylamide hydrogels are not stable in saline solutions: upon the immersion in saline solution, the alginate network will dissociate as the ionic crosslinkers (calcium ions) exchange with external ions (e.g., sodium ions).[48] It will be interesting to use our method to print other hydrogels, but here we will focus on the development of the method itself by using the microgel-reinforced hydrogel. This microgel-reinforced hydrogel has high fracture energy,[49] is stable in saline solutions,[26,50] and has been used in cast,[49,51] dip coat,[26] and print.[52] We prepare the microgels (Figure S1, Supporting Information) and add them to the precursor of the matrix hydrogel (i.e., an aqueous solution of monomer (acrylamide), crosslinker (*N*,*N*′-methylenebis(acrylamide), MBAA), and initiator (α-ketoglutaric) for radical polymerization). A nanoclay is used as a rheological modifier to turn the ink into a plastic liquid (Figure S2a–c, Supporting Information). Laponite nanoclays are nanoscale silicate platelets with positive charges on the edges and negative charges on the faces. This charge distribution leads to a stable "house-of-cards" structure in an aqueous suspension of Laponite, which is self-supporting and only flows when the shear stress is above the yield stress.[53] The ink is printable for appropriate combinations of the concentrations of the microgel and nanoclay (Figure S2d, Supporting Information). Prints are achieved in a wide range of resolutions; our thinnest print is 260 μm (Figure S2e, Supporting Information). The ink retains the shape in an angle of 90° for 4 h, whereas the ink without the nanoclay drips (Figure S2f, Supporting Information). We prepare the ink for a silicone elastomer using nanosilica as the rheological modifier.[54,55] To

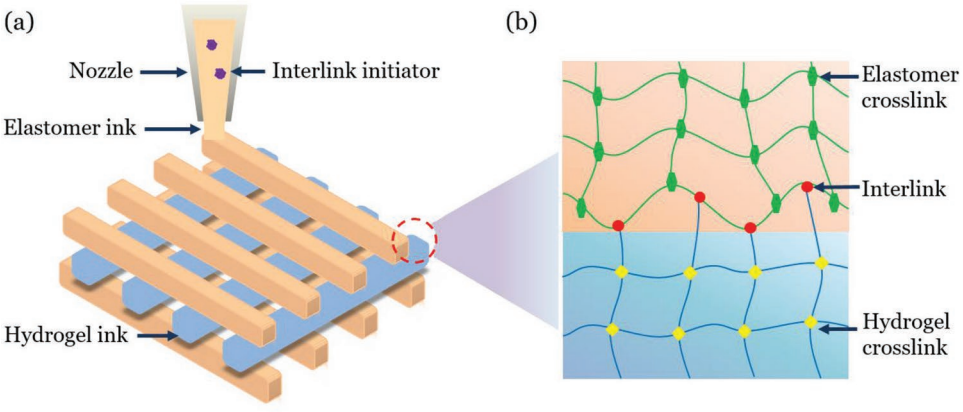

Figure 1. An approach to print integrated structures of a hydrogel and an elastomer, in arbitrary sequence, and with strong adhesion. a) During print, the two inks are extruded in arbitrary sequence and retain shape against gravity and capillarity. The elastomer ink carries the interlink initiator. b) During cure, the covalent crosslinks form within each network and covalent interlinks form between the two networks.

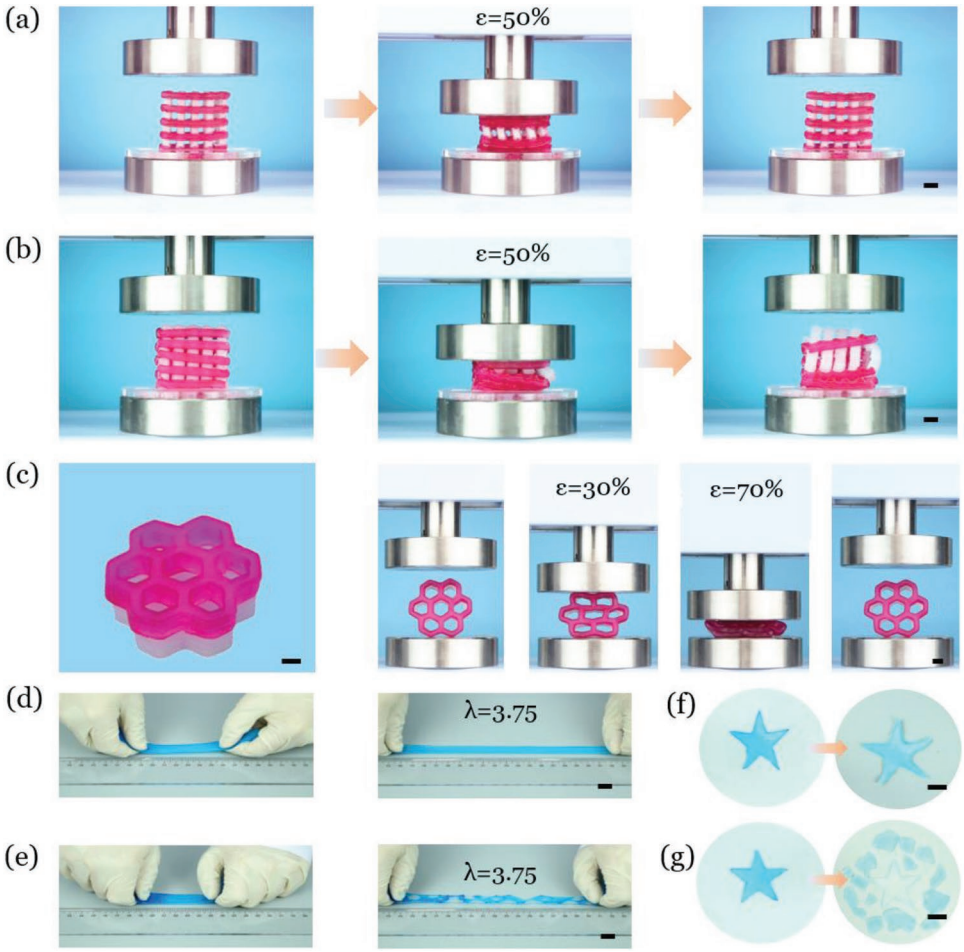

Figure 2. The mechanical behavior of cured prints. After cure, the hydrogel is dyed in red or blue to help visualization. a) A hydrogel–elastomer lattice with covalent interlinks endures compression and recovers the original shape. b) A hydrogel–elastomer lattice without covalent interlinks debonds under compression and does not recover the original shape. c) A hydrogel–elastomer honeycomb with covalent interlinks buckles under compression but remains adherent. d) The bilayer of the microgel-reinforced hydrogel and elastomer endures a large stretch. e) The bilayer of the PNaAMPS hydrogel and the elastomer ruptures and debonds. When immersed in deionized water, f) the bilayer with the microgel-reinforced hydrogel bends due to swelling but g) the bilayer with the PNaAMPS hydrogel ruptures and debonds. All scale bars are 1 cm.

the elastomer ink we also add a photoinitiator (benzophenone), which, during cure, will induce the formation of interlinks between the elastomer and the hydrogel (Figure S3, Supporting Information). The printed structures retain shape during 4 h of cure, in a glove box of argon atmosphere, under UV irradiation.

We ascertain the quality of the cured prints through their mechanical behavior. With the interlink initiator, a hydrogel–elastomer lattice does not debond under compression and recovers the initial shape (**Figure 2**a and Movie S1, Supporting Information). Without the interlink initiator, a hydrogel–elastomer lattice debonds under compression and does not recover the initial shape (Figure 2b). The difference is also observed under tension (Figure S4, Supporting Information). We also print an interlinked hydrogel–elastomer honeycomb (Figure 2c). Under compression, the honeycomb buckles but remains adherent. A bilayer of the elastomer and the microgel-reinforced hydrogel survives stretch (Figure 2d). A bilayer of the elastomer and the PNaAMPS hydrogel ruptures and debonds (Figure 2e). When submerged in deionized water for 100 min, the former swells and bends (Figure 2f) but the latter ruptures and debonds (Figure 2g).

A microgel-reinforced hydrogel ruptures at a stretch of 16.1, an elastomer ruptures at a stretches of 12.8, and a hydrogel–elastomer hybrid ruptures at a stretch of 8.4 (**Figure 3**a). The hybrid ruptures at a stress of 0.6 MPa. Another hybrid hangs a basket without failure (Figure S5, Supporting Information). The hydrogels have fracture energy above 5000 J m^{-2}, increasing with the concentration of the nanoclay (Figure 3b). The values of fracture energies reported here are among the highest of all hydrogels, printed or fabricated by other means. Our prints have achieved comparable values of fracture energy for the hydrogel (with 1 wt% of nanoclay), elastomer, and hybrid (Figure 3c). The fracture energy of the hybrid is as high as 5506 ± 874 J m^{-2}. This value is determined in a pure shear test, where a precut crack on the interface, upon loading, blunts and kinks into the hydrogel (Figure 3d). The measured fracture energy is taken to be a lower bound of the adhesion energy.

The photoinitiator (benzophenone) not only induces hydrogel–elastomer interlinks but also affects the mechanical behavior of the cured elastomer. The photoinitiator has long been used to modify the surface of the elastomer and the

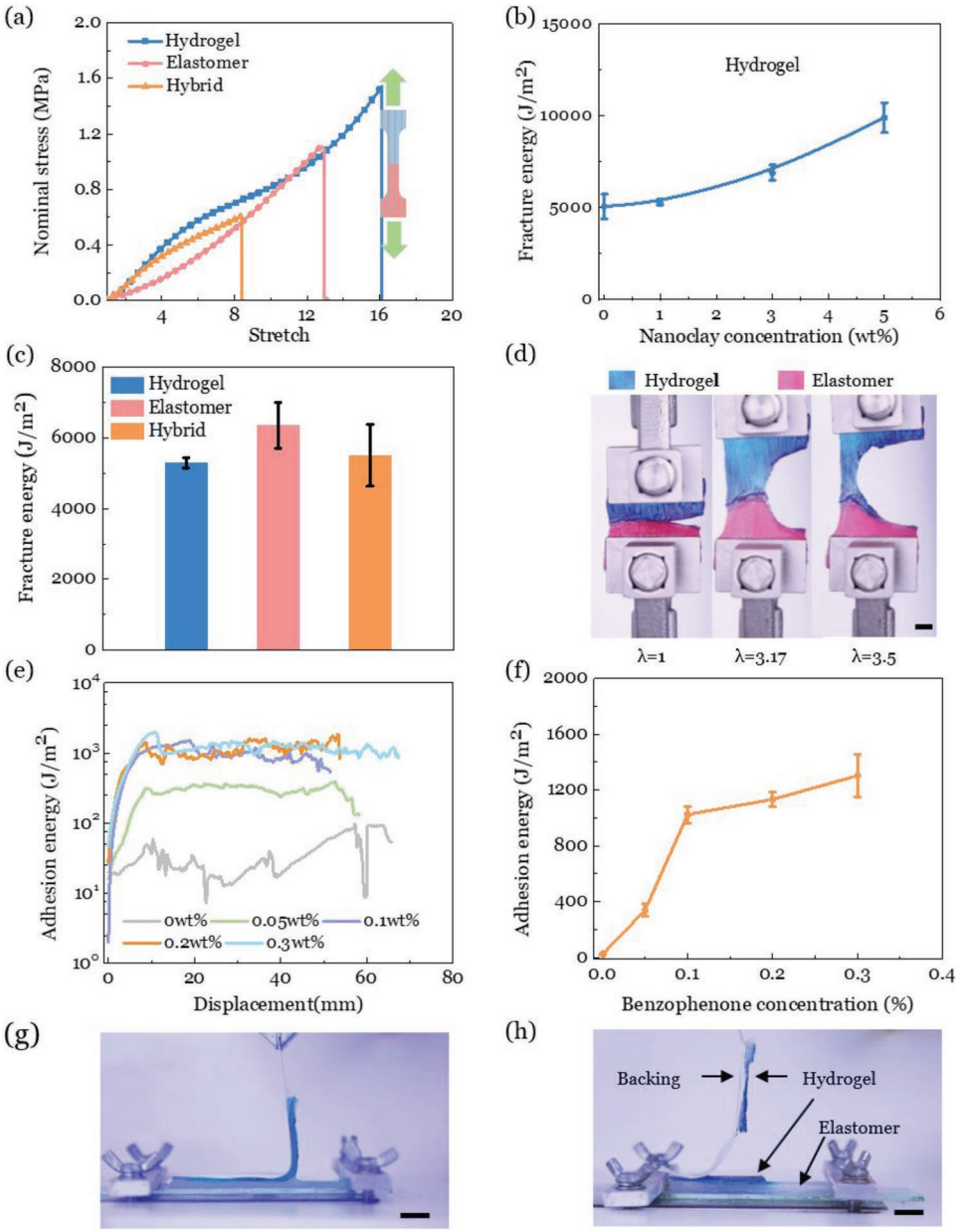

Figure 3. a) The stress–stretch curves of the printed hydrogel (with 1 wt% of nanoclay), elastomer, and hybrid. The hybrid is stretched in the direction normal to the interface. b) The fracture energy of the printed hydrogel is a function of the concentration of nanoclay. The hydrogel of no nanoclay could not be printed and was cast. c) The fracture energies of printed hydrogel (1 wt% of nanoclay), elastomer, and hybrid. d) Images for the pure shear test of the hybrid. e) Recorded relations between peeling force and peeling displacement. A plateau corresponds to steady peeling and gives the adhesion energy. f) The adhesion energy as a function of the concentration of benzophenone. g) Peel by adhesive failure. h) Peel by cohesive failure. The scales bars are 1 cm.

affected zone is limited to a region of some depth beneath the surface; the effect of the surface modification on the mechanical behavior has yet been characterized.[27,41,56,57] Here we use the photoinitiator to modify the entire volume of the elastomer ink, and the effect of the photoinitiator of the mechanical behavior is readily characterized by measuring the stress–stretch curves of the cured elastomer (Figure S6, Supporting Information). The photoinitiator changes the stress–stretch curves somewhat. The mechanism of this change may deserve a study for its own sake, but this change should not cause concern for print in practice. Desired properties of the ink and cured prints can be achieved by tuning independent variables, such as the concentrations of the rheological modifier, crosslink agent, and interlink initiator.

A printed structure inevitably has defects, which often lower its mechanical performance.[58,59] However, our prints have high enough fracture/adhesion energy to ensure defect tolerance. For a representative value of facture/adhesion energy of 1000 J m^{-2}, along with a work of fracture (i.e., the area under the stress–stretch curve up to fracture of an uncut sample) of 10^7 J m^{-3},

their ratio defines a length scale of 0.1 mm. Defects below this length scale do not lower the stretchability of the structure.[60]

The mechanical behavior of the printed hydrogels and elastomers is comparable to that of their cast counterparts (Figure S7a–c, Supporting Information). A concern is commonly raised that a structure behaves differently in the printing direction and the perpendicular direction.[58,61–63] However, our prints show little directional dependence (Figure S7d–f, Supporting Information).

The adhesion energy between the hydrogel and elastomer increases with the concentration of the interlink initiator (Figure 3e,f). We observe both adhesive and cohesive failure (Figure 3g,h). The adhesion energy is too high to measure by the peeling test when the concentration of the interlink initiator is above 0.3 wt% because the cyanoacrylate used to glue the inextensible backing layer debonds.[27,42]

Hydrogels have long been used to make stimuli-responsive morphing structures.[64] Here we print tough and adherent ones. We print a hydrogel–elastomer flower and a butterfly (**Figure 4**a,b). Upon immersion in deionized water, the hydrogel swells but the elastomer does not, so that the flower morphs. We also print a hydrogel–elastomer octopus and its tentacles bend upon swelling (Figure 4c). We print two hydrogel dolphins, one being naked and the other being coated by the elastomer. In the open air, the naked dolphin loses ≈60% of its weight in 2 d (Figure 4d), but the coated dolphin does not lose weight appreciably (Figure 4e and Figure S8, Supporting Information). Hydrogel containing hygroscopic salts and with hydrophobic coats can enable devices that one can wear, wash, and iron.[28,42]

As noted in the beginning of this paper, integrated hydrogels and elastomers are under rapid development as soft ionic devices.[2,3] Here we print a tough and adherent artificial axon (**Figure 5**a). The artificial axon transmits music signals from a cell phone to a loudspeaker (Figure 5b). The capacitance of the artificial axon increases linearly with the stretch and matches well with the theoretical prediction, $C = C_0\lambda$ (Figure 5c). We also cyclically stretch the artificial axon with a maximum strain of 8% at a frequency of 1 Hz. The capacitance changes simultaneously with the deformation and shows no change after 100 cycles (Figure 5d). Subject to stretch and twist, an artificial axon with strong adhesion remains intact (Figure 5e), but an artificial axon with weak adhesion readily debonds (Figure 5f). The tough and adherent artificial axon survives repeated hits by a hammer (Figure 5g), and the change in capacitance is recorded (Figure 5h and Movie S2, Supporting Information). The artificial axon still transmits musical signal well after repeated hits by a hammer (Movie S3, Supporting Information).

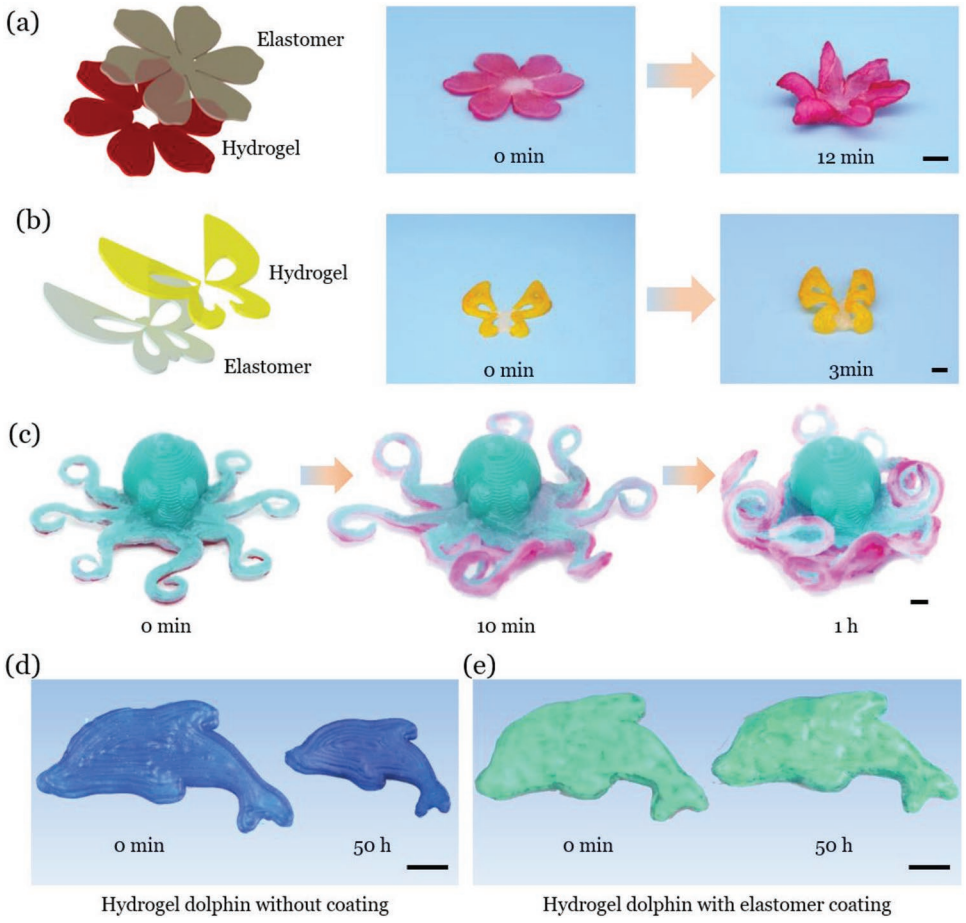

Figure 4. Tough and adherent stimuli-responsive morphing structures. a) A hydrogel–elastomer flower and b) butterfly morphs in deionized water. c) A hydrogel–elastomer octopus bends its tentacles in deionized water. d) In open air, a naked hydrogel dolphin loses water substantially but e) an elastomer-coated one does not. The scale bars are 1 cm.

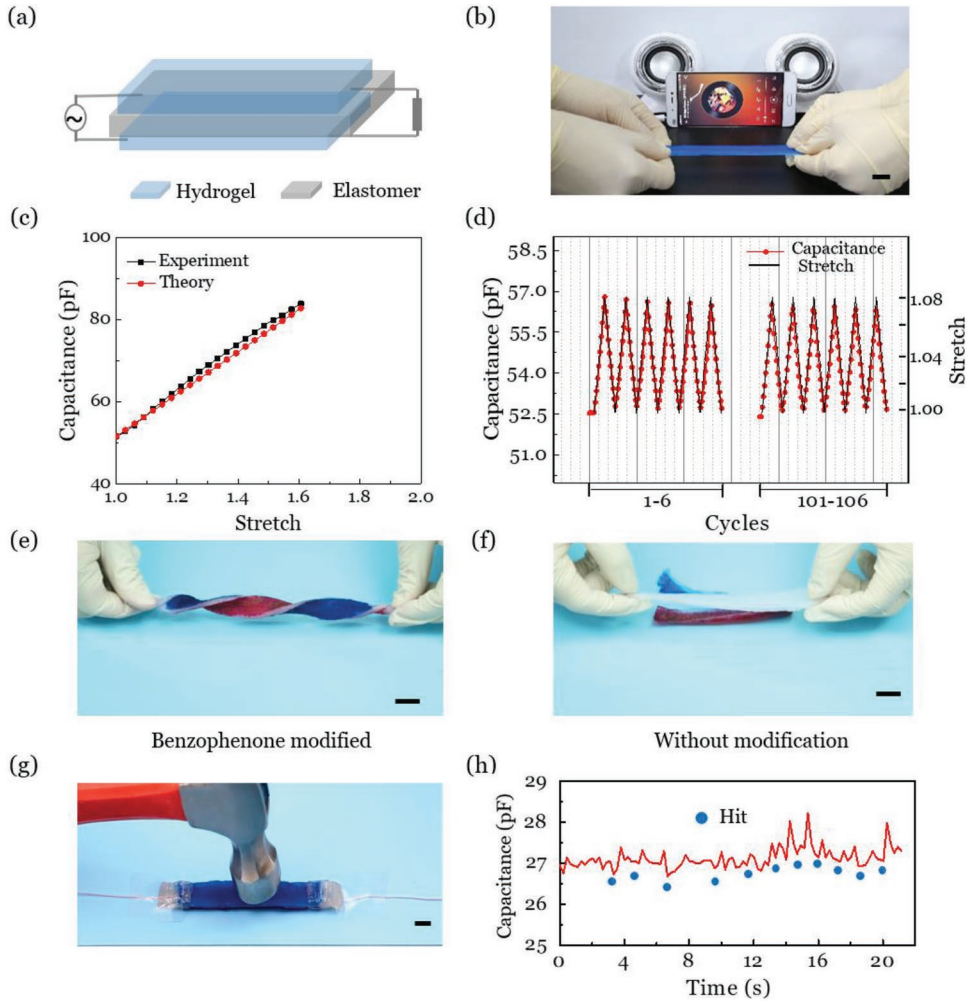

Figure 5. Tough and adherent artificial axon. a) An artificial axon consists of an elastomer sandwiched between two hydrogels, and functions as a transmission line of electrical signals. b) The artificial axon transmits music signals under stretch. c) The experimental and theoretical relations between the capacitance and stretch. d) The artificial axon also functions as a capacitive strain sensor. The signals are repeatable after 100 cycles of stretching. e) An artificial axon with strong adhesion endures stretch and twist. f) An artificial axon with weak adhesion debonds easily. g) While a tough and adherent artificial axon is hit repeatedly by a hammer, h) the electrical signal is recorded. The scale bars are 1 cm.

3. Conclusion

In summary, we have described an approach to print integrated structures of a hydrogel and an elastomer, in arbitrary sequence, with strong adhesion. We have demonstrated this approach with a specific set of chemistries that leads to unusually high adhesion energy, above 5000 J m^{-2}. The approach can be readily adapted to many other hydrogels and hydrophobic elastomers. For example, many devices use polyacrylamide hydrogels, which has fracture energy on the order of 100 J m^{-2}. Our approach will readily generate sparse covalent interlinks between the hydrogel and the elastomer to achieve adhesion energy comparable to the fracture energy of the hydrogel. To induce the formation of hydrogel–elastomer interlinks, we have added a photoinitiator to the elastomer ink, but thermoinitiators may also be used. The rheology of the precursors can also be tuned to enable other fabrication processes, such as dip coating an object of an arbitrary shape with alternating layers of elastomer and hydrogel. It is hoped that the approach will enable the rapid prototyping of soft devices for broad applications in medicine and engineering.

4. Experimental Section

Materials: 2-Acrylamido-2-methyl-1-propanesulfonic acid sodium salt (NaAMPS; Sigma-Aldrich 655821), MBAA (Aladdin M128783), α-ketoglutaric acid (Aladdin K105571), acrylamide (AAm; Aladdin A108467), ecoflex (Smooth-on, 00-30), benzophenone (Aladdin B103862), Laponie XLG (BYK Additives and Instruments, Germany), nanosilica (15 nm, Aladdin S104600), Rain-x (ITW Inc.), RTV adhesive (Ausbond), and cyanoacrylate (Loctite 406, Henkel) were purchased. All chemicals were used as purchased without any further purification.

Preparation of the Microgels: A solution was prepared using deionized water, 1 M of NaAMPS (monomer), 4 mol% MBAA (crosslinker) relative to the monomer, and 0.1 mol% of α-ketoglutaric acid (initiator) relative to the monomer. The solution was poured into a mold made of a glass plate and a 9 mm silicone spacer and cured in argon atmosphere for 8 h using the 365 nm UV light with the intensity of 2.5 mW cm^{-2}. The hydrogel was freeze-dried for 2 d in a lyophilizer

(FD-1A-80, Boyikang Inc.). The freeze-dried particles were grinded into fine powders in a planetary grinder (DECO-PBM-V-0.4L) for 12 h and then filtrated with a standard sifter (50 in mesh number). The granularity distribution of the powders was measured by a particle size analyzer (LS-909, OMEC MOTORS). The powders were kept dry before use.

Preparation of the Microgel-Reinforced Hydrogel Ink: A solution was prepared by deionized water, 4 M of AAm (monomer), 0.001 mol% MBAA relative to the monomer, and 0.02 mol% of α-ketoglutaric acid relative to the monomer. A nanoclay (Laponite XLG)) of a certain concentration (between 1 and 5 wt% in the precursor) was mixed in the solution by magnetic stirring for 24 h. The microgels were added to the mixture at required concentrations (1, 3, and 5 wt%) and then mixed and degassed with a planetary mixer (Thinky ARE-300) at 2000 RPM for 2 min. The mixture was stored at 2–8 °C for 2 d to guarantee the fully swelling of the microgels without decomposing α-ketoglutaric acid. The mixture was stirred for more than two times to form homogeneous pasty ink before print.

Preparation of the Elastomer Ink: The precursor of the elastomer (Ecoflex) has two liquids: a base (part A) and a cure agent (part B). Benzophenone was mixed with part A and then the mixture were heated in an oven of 60 °C for 30 min to dissolve benzophenone. After the solution was cooled to room temperature, part B was added (A: B at 1:1 in weight), along with nanosilica (3–5 wt% of the weight of Ecoflex). The mixture was mixed in a planetary mixer (Thinky ARE-300) at 2000 RPM and degassed at 2200 RPM for 2 min before print.

Rheological Characterization: All the rheological measurements were carried out using the Anton Paar MCR302 Rheometer. Oscillatory rheometry was performed for the hydrogel ink (2.5 wt% microgel, 3 wt% nanoclay as a typical ink) with a frequency of 1 Hz and oscillating stress of 1–1000 Pa. Viscometry was performed for the hydrogel ink with 2.5 wt% microgel and 0, 1, 3, and 5 wt% nanoclay in plate geometry with shear rate of 0.01–1000 s^{-1}.

Print of Hydrogel–Elastomer Hybrid: The printer was modified from a MakerBot Replicator 2X. An air bump system (OTS-800-30L and AD-982) was set up to extrude the inks of the hydrogel and the elastomer. For the items in Figures 2,4, and 5, the two materials were printed one by one without any interval. 5 wt% nanoclay for the hydrogel and 5 wt% nanosilica for the elastomer were used to provide suitable rheology to print the hybrid lattices (Figure 2a,b) and the artificial axon (Figure 5). 1 wt% nanoclay for the hydrogel and 4 wt% nanosilica for the elastomer were used to print the laminates (Figure 2c–g), flower, butterfly, octopus, and dolphin (Figure 4). For tensile, pure shear and 90° peeling test specimens in Figure 3, 1 wt% nanoclay for the hydrogel and 4 wt% nanosilica for the elastomer were used. The elastomer was also printed and let it cure at room temperature for 2 h, and the hydrogel was printed on or next to the elastomer. All these items were printed in open air and cured in argon atmosphere using the 365 nm UV light with intensity of 2.5 mW cm^{-2} for 4 h.

Mechanical Tests: Samples were prepared to compare the mechanical behavior of casts and prints. The hydrogel was cast in two pieces of glass washed by Rain-x previously with 1 mm spacer and then cured in argon atmosphere using the 365 nm UV with intensity of 2.5 mW cm^{-2} for 4 h. The elastomer was cast between two pieces of acrylic sheets. A 100 mm × 120 mm sheet was printed on glass plates and UV irradiated for 4 h. For the tensile test, the samples were cut into a dumbbell shape with 2 mm in width and 12 mm in gauge length. For the pure shear test, a rectangle of 50 mm × 30 mm was cut with a laser cutter and a crack of 20 mm was cut in the middle. For the 90° peeling test, the elastomer was bonded to a 2 mm glass sheet by Ausbond RTV adhesive, and the hydrogel was bonded to a paper as the backing layer (Double A, A4 80G) by cyanoacrylate (Loctite 406). The tensile and pure shear tests were performed by a tensile machine (SMADAZU AGS-X) with a velocity of 50 mm min^{-1}. The 90° peeling test was performed by a peeling machine (MK-BL-X) with a velocity of 50 mm min^{-1}.

Electrical Measurement: All the electrical measurements were performed by an impedance analyzer WK 6500B. The capacitance was measured under 1 kHz. The stretch was applied by a tensile machine (SMADAZU AGS-X) with a velocity of 30 mm min^{-1}.

Photos and Videos: All photos and videos are taken by Cannon GI 890 (Cannon).

Supporting Information

Supporting Information is available from the Wiley Online Library or from the author.

Acknowledgements

H.Y., C.L., and M.Y. contributed equally to this work. This research was supported by the Harvard University Materials Research Science and Engineering Center (DMR-14-20570), and National Natural Science Foundation of China (No. 11702208), and the Program for Postdoctoral Innovative Talents (No. BX201700192).

Conflict of Interest

The authors declare no conflict of interest.

Keywords

3D printing, hydrogel–elastomer hybrids, soft devices, strong adhesion

Received: February 25, 2019
Published online:

[1] P. Dayan, L. F. Abbott, L. Abbott, *Theoretical Neuroscience: Computational and Mathematical Modeling of Neural Systems* **2001**.
[2] H. R. Lee, C. C. Kim, J. Y. Sun, *Adv. Mater.* **2018**, *30*, e1704403.
[3] C. H. Yang, Z. G. Suo, *Nat. Rev. Mater.* **2018**, *3*, 125.
[4] C. Keplinger, Z. Suo, *Science* **2013**, *341*, 984.
[5] P. Rothemund, X. P. Morelle, K. Jia, G. M. Whitesides, Z. G. Suo, *Adv. Funct. Mater.* **2018**, *28*, 1800653.
[6] N. Kellaris, V. G. Venkata, G. M. Smith, S. K. Mitchell, C. Keplinger, *Sci. Rob.* **2018**, *3*, eaar3276.
[7] E. Acome, S. Mitchell, T. Morrissey, M. Emmett, C. Benjamin, M. King, M. Radakovitz, C. Keplinger, *Science* **2018**, *359*, 61.
[8] C. H. Yang, B. Chen, J. L. Jing, H. Y. Jian, J. Zhou, M. C. Yong, Z. Suo, *Extreme Mech. Lett.* **2015**, *3*, 59.
[9] D. Espinosahoyos, A. Jagielska, K. A. Homan, H. Du, T. Busbee, D. G. Anderson, N. X. Fang, J. A. Lewis, K. J. V. Vliet, *Sci. Rep.* **2018**, *8*, 478.
[10] J. Y. Sun, C. Keplinger, G. M. Whitesides, Z. Suo, *Adv. Mater.* **2014**, *26*, 7608.
[11] C. H. Yang, B. Chen, J. Zhou, Y. M. Chen, Z. Suo, *Adv. Mater.* **2016**, *28*, 4480.
[12] C. Larson, B. Peele, S. Li, S. Robinson, M. Totaro, L. Beccai, B. Mazzolai, R. Shepherd, *Science* **2016**, *351*, 1071.
[13] C. C. Kim, H. H. Lee, K. H. Oh, J. Y. Sun, *Science* **2016**, *353*, 682.
[14] M. S. Sarwar, Y. Dobashi, C. Preston, J. K. Wyss, S. Mirabbasi, J. D. W. Madden, *Sci. Adv.* **2017**, *3*, e1602200.
[15] W. Xu, L. B. Huang, M. C. Wong, L. Chen, G. Bai, J. Hao, *Adv. Energy Mater.* **2017**, *7*, 1601529.
[16] X. Pu, M. Liu, X. Chen, J. Sun, C. Du, Y. Zhang, J. Zhai, W. Hu, Z. L. Wang, *Sci. Adv.* **2017**, *3*, e1700015.
[17] K. Parida, V. Kumar, W. Jiangxin, V. Bhavanasi, R. Bendi, P. S. Lee, *Adv. Mater.* **2017**, *29*, 1702181.

[18] Y. Lee, S. H. Cha, Y. W. Kim, D. Choi, J. Y. Sun, *Nat. Commun.* **2018**, *9*, 1804.
[19] C. H. Yang, S. Zhou, S. Shian, D. R. Clarke, Z. Suo, *Mater. Horiz.* **2017**, *4*, 1102.
[20] T. Li, G. Li, Y. Liang, T. Cheng, J. Dai, X. Yang, B. Liu, Z. Zeng, Z. Huang, Y. Luo, *Sci. Adv.* **2017**, *3*, e1602045.
[21] R. Langer, *Nature* **1998**, *392,* 5.
[22] T. R. Hoare, D. S. Kohane, *Polymer* **2008**, *49*, 1993.
[23] X. Liu, T.-C. Tang, E. Tham, H. Yuk, S. Lin, T. K. Lu, X. Zhao, *Proc. Natl. Acad. Sci. USA* **2017**, *114*, 2200.
[24] G. A. Parada, H. Yuk, X. Liu, A. J. Hsieh, X. Zhao, *Adv. Healthcare Mater.* **2017**, *6*, 1700520.
[25] Y. Yu, H. Yuk, G. A. Parada, Y. Wu, X. Liu, C. S. Nabzdyk, K. Youcef-Toumi, J. Zang, X. Zhao, *Adv. Mater.* **2019**, *31*, 1807101.
[26] R. Takahashi, K. Shimano, H. Okazaki, T. Kurokawa, T. Nakajima, T. Nonoyama, D. R. King, J. P. Gong, *Adv. Mater. Interfaces* **2018**, *5*, 1801018.
[27] H. Yuk, T. Zhang, G. A. Parada, X. Liu, X. Zhao, *Nat. Commun.* **2016**, *7*, 12028.
[28] P. Le Floch, X. Yao, Q. H. Liu, Z. J. Wang, G. D. Nian, Y. Sun, L. Jia, Z. G. Suo, *ACS Appl. Mater. Interfaces* **2017**, *9*, 25542.
[29] R. L. Truby, J. A. Lewis, *Nature* **2016**, *540*, 371.
[30] X. Kuang, D. J. Roach, J. Wu, C. M. Hamel, Z. Ding, T. Wang, M. L. Dunn, H. J. Qi, *Adv. Funct. Mater.* **2019**, *29*, 1805290.
[31] T. J. Wallin, J. Pikul, R. F. Shepherd, *Nat. Rev. Mater.* **2018**, *3*, 84.
[32] J. P. Gong, Y. Katsuyama, T. Kurokawa, Y. Osada, *Adv. Mater.* **2003**, *15*, 1155.
[33] R. Bai, J. Yang, Z. Suo, *Eur. J. Mech.-A/Solids* **2019**, *74*, 337.
[34] C. Creton, *Macromolecules* **2017**, *50*, 8297.
[35] J.-Y. Sun, X. Zhao, W. R. Illeperuma, O. Chaudhuri, K. H. Oh, D. J. Mooney, J. J. Vlassak, Z. Suo, *Nature* **2012**, *489*, 133.
[36] J. Tang, J. Li, J. J. Vlassak, Z. Suo, *Soft Matter* **2016**, *12*, 1093.
[37] K. Efimenko, W. E. Wallace, J. Genzer, *J. Colloid Interface Sci.* **2002**, *254*, 306.
[38] D. Hegemann, H. Brunner, C. Oehr, *Nucl. Instrum. Methods Phys. Res., Sect. B* **2003**, *208*, 281.
[39] D. Bodas, C. Khan-Malek, *Sens. Actuators, B* **2007**, *123*, 368.
[40] C. Cha, E. Antoniadou, M. Lee, J. H. Jeong, W. W. Ahmed, T. A. Saif, S. A. Boppart, H. Kong, *Angew. Chem.* **2013**, *125*, 7087.
[41] G. Haghiashtiani, E. Habtour, S.-H. Park, F. Gardea, M. C. McAlpine, *Extreme Mech. Lett.* **2018**, *21*, 1.
[42] Q. Liu, G. Nian, C. Yang, S. Qu, Z. Suo, *Nat. Commun.* **2018**, *9*, 846.
[43] K. Tian, J. Bae, S. E. Bakarich, C. Yang, R. D. Gately, G. M. Spinks, H. P. M. In, Z. Suo, J. J. Vlassak, *Adv. Mater.* **2017**, *29*, 1604827.
[44] B. Zhang, S. Y. Li, H. Hingorani, A. Serjouei, L. Larush, A. A. Pawar, W. H. Goh, A. H. Sakhaei, M. Hashimoto, K. Kowsari, S. Magdassi, Q. Ge, *J. Mater. Chem. B* **2018**, *6*, 3246.
[45] H. Zhang, X. Guo, J. Wu, D. Fang, Y. Zhang, *Sci. Adv.* **2018**, *4*, eaar8535.
[46] B. Chen, W. Tang, T. Jiang, L. Zhu, X. Chen, C. He, L. Xu, H. Guo, P. Lin, D. Li, *Nano Energy* **2018**, *45*, 380.
[47] S. E. Bakarich, S. Beirne, G. G. Wallace, G. M. Spinks, *J. Mater. Chem. B* **2013**, *1*, 4939.
[48] J. Y. Li, Z. G. Suo, J. J. Vlassak, *J. Mater. Chem. B* **2014**, *2*, 6708.
[49] J. Hu, K. Hiwatashi, T. Kurokawa, S. M. Liang, Z. L. Wu, J. P. Gong, *Macromolecules* **2011**, *44*, 7775.
[50] C. Azuma, K. Yasuda, Y. Tanabe, H. Taniguro, F. Kanaya, A. Nakayama, Y. M. Chen, J. P. Gong, Y. Osada, *J. Biomed. Mater. Res., Part A* **2007**, *81*, 373.
[51] J. Saito, H. Furukawa, T. Kurokawa, R. Kuwabara, S. Kuroda, J. Hu, Y. Tanaka, J. P. Gong, N. Kitamura, K. Yasuda, *Polym. Chem.* **2011**, *2*, 575.
[52] H. Furukawa, M. Kawakami, J. Gong, M. Makino, M. H. Kabir, A. Saito, *3-D Gel Printing for Soft-matter Systems Innovation*, presented at *Nanosensors, Biosensors, & Info-tech Sensors & Systems*, San Diego, California, USA, April **2015**.
[53] Y. Jin, C. Liu, W. Chai, A. Compaan, Y. Huang, *ACS Appl. Mater. Interfaces* **2017**, *9*, 17456.
[54] Y. Kim, H. Yuk, R. Zhao, S. A. Chester, X. Zhao, *Nature* **2018**, *558*, 274.
[55] J. A. Lewis, *Adv. Funct. Mater.* **2006**, *16*, 2193.
[56] W. Yuli, L. Hsuan-Hong, B. Mark, C. E. Sims, G. P. Li, N. L. Allbritton, *Anal. Chem.* **2005**, *77*, 7539.
[57] H. Shuwen, R. Xueqin, B. Mark, C. E. Sims, G. P. Li, N. L. Allbritton, *Anal. Chem.* **2004**, *76*, 1865.
[58] J. R. C. Dizon, A. H. Espera, Q. Chen, R. C. Advincula, *Addit. Manuf.* **2018**, *20*, 44.
[59] B. Caulfield, P. McHugh, S. Lohfeld, *J. Mater. Process. Technol.* **2007**, *182*, 477.
[60] C. Chao, Z. Wang, Z. Suo, *Extreme Mech. Lett.* **2017**, *10*, 50.
[61] Z. Quan, J. Suhr, J. Yu, X. Qin, C. Cotton, M. Mirotznik, T.-W. Chou, *Compos. Struct.* **2018**, *184*, 917.
[62] W. Wu, P. Geng, G. Li, D. Zhao, H. Zhang, J. Zhao, *Materials* **2015**, *8*, 5834.
[63] R. Zaldivar, D. Witkin, T. McLouth, D. Patel, K. Schmitt, J. Nokes, *Addit. Manuf.* **2017**, *13*, 71.
[64] D. J. Beebe, J. S. Moore, J. M. Bauer, Q. Yu, R. H. Liu, C. Devadoss, B.-H. Jo, *Nature* **2000**, *404*, 588.